An Improved Natural Frequency Based Line Fault Location Method on Untransposed Lines

Yuan Nie[1], *Student Member, IEEE*, Yu Liu[1,2,*], *Member, IEEE*, Xiaodong Zheng[2,3], *Member, IEEE*, and Dayou Lu[1], *Student Member, IEEE*

1. School of Information Science and Technology, ShanghaiTech University, Shanghai, China, 201210
2. Key Laboratory of Control of Power Transmission and Conversion, Ministry of Education, Shanghai, China, 200240
3. Department of Electrical Power Engineering, Shanghai Jiao Tong University, Shanghai, China, 200240

* Email: liuyu.shanghaitech@gmail.com

***Abstract*— Accurate fault location method reduces power outage time and operational costs. In this paper, a novel natural frequency based fault location method is proposed for untransposed transmission lines. The new method is without the assumption that the transmission line is geometrically symmetrical by reconstructing the new phase to model transformation matrix. The connections of mode networks during faults with the new transformation matrix are also derived, to ensure validity of the fault location method. Numerical experiments prove that the proposed fault location approach presents higher fault location accuracy compared to existing natural frequency based fault location method during phase faults with different fault types, locations and impedances.**

***Index Terms*—fault location, natural frequency, untransposed lines, phase to model transformation**

I. Introduction

Accurate fault location method is valuable for reducing the power outage time and operating costs of the power system. Fault location methods of transmission lines have received widespread attention in literatures. Existing fault location methods can be mainly divided into fault analysis based methods and traveling wave based methods.

A. Fault analysis based methods

Fault analysis based methods calculate the distance between one terminal and the fault location by constructing the relationship of voltages and currents at the measure terminal using the relevant parameters of the transmission line. Fault analysis based method can be further classified into single-ended method and dual-ended method.

Single-ended method calculates the fault distance by using one-end current and voltage measurements to compute the distance between the fault location and the measurement. The main advantage of single ended method is not requiring the communication from the remote terminal and the measurement terminal which can be simpler and more economical comparing with dual-ended methods. But the disadvantage of single-ended method is that the accuracy is affected by many factors such as fault impedances and source impedances [1].

The dual-ended methods are developed to overcome the limitation of the single ended method. Dual-ended method use voltages and currents at both ends of the transmission line. The physical relationship among measured voltages, measured currents and fault location can be expressed either using phasor domain [2] or time domain [3,4] expressions. As these methods using two ends information to calculated the fault distance, dual-ended method is typically not affected by the source impedance and fault impedance. However, for dual-ended method, it is necessary to obtain the voltage and current information from the other end, so these methods require communication channels from the other end. The dual-ended method is also divided into GPS synchronized and non-synchronized methods [5].

This work is sponsored by National Nature Science Foundation of China (No. 51807119), Shanghai Pujiang Program (No. 18PJ1408100) and Key Laboratory of Control of Power Transmission and Conversion (SJTU), Ministry of Education (No. 2015AB04). Their support is greatly appreciated.

B. Traveling wave based method

When a fault occurs on the transmission line, high frequency traveling waves are generated on the transmission line and reflected between terminals and the fault location. Traveling wave based methods monitor the traveling waves at one or both ends of the line. In these methods, the fact that the traveling time is proportional to the fault location is used to determine the fault location. Single ended methods [6] utilize subsequent wavefront arrival time at the local terminal of the line to determine the fault locaiton, include the type A, C, E and F fault locators. Dual-ended methods [7,8] such as type B and D fault locators detect the arrival of the first wavefront at both sides then use the arrival time difference to calculated the fault location. The effectiveness of the traveling wave based approaches highly depends on the reliable detection of wavefronts. However, the detection reliability may be compromised especially during faults with small inception angles or faults with gradually changing fault resistance.

Natural frequency based fault location approaches have been adopted in both HVDC [9] and HVAC [10] systems in recent years. The main idea is to use the information embedded in the traveling-wave spectrum: the dominant frequency is proportional to the reciprocal of the location of the fault. These methods only require local information (single-ended approaches) and do not require reliable detection of wavefronts. When applied to AC systems, Clarke transformation is usually utilized to transform the phase network into decoupled mode networks and to find the fault location. However, when applied to untransposed lines in AC systems, Clarke transformation may not be able to fully decouple the three phase transmission lines, which may bring errors for the existing natural frequency based fault location approaches.

C. Proposed method

In this paper, an improved natural frequency based line fault location method in untransposed lines is proposed. To fully decouple the three phase transmission line into three independent single mode networks, unlike the existing method which utilizes Clarke transformation to decouple the three phase transmission line, the proposed method reconstruct a general transformation matrix that works with asymmetrical tower structures and arbitrary parameters. Without the symmetry assumption, more accurate wave speed and mode networks during faults can be obtained by using the new transformation matrix. Consequently, the proposed method has higher accuracy compared to the existing method. The remainder of the paper is arranged as follows. Section II reviews the existing natural frequency based fault location approach. Section III introduces the proposed method by constructing a new transformation matrix and deriving the connections of mode networks during faults with the new transformation matrix. Section IV verifies the effectiveness of the proposed method through the numerical experiments. Section VI draws a conclusion.

978-1-7281-5748-1/20/$31.00 ©2020 IEEE

II. Review of The Existing Natural Frequency Based Fault Location Method

This section reviews the existing natural frequency based fault location method. First, the three phase transmission line is modeled using partial differential equations and is decoupled into different modes using Clarke transformation. Second, the natural frequency based fault location approach on the mode network is introduced.

A. Modeling and decoupling of three phase transmission lines

A fault will generate the traveling waves along the transmission line, which will reflect and transmit at each discontinuity of the line. The traveling wave propagation can be described by partial differential equations. Here, a three phase lossless transmission line is taken as an example as shown in Figure 1. $u_m(x,t)$ and $i_m(x,t)$ ($m=a,b,c$) are per phase voltages and currents on the transmission line at the location x. The matrices L and C are the inductance and capacitance matrices per unit length. The length of the overall transmission line is l.

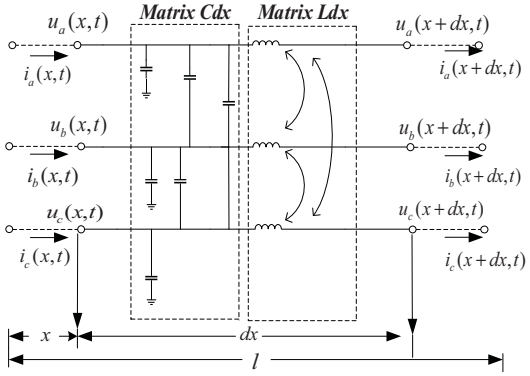

Figure.1 The three phase lossless transmission line model

The partial differential equations representing this model are,

$$\begin{cases}\partial^2 \boldsymbol{u}_{abc}(x,t)/\partial x^2 = \boldsymbol{LC}\partial^2 \boldsymbol{u}_{abc}(x,t)/\partial t^2 \\ \partial^2 \boldsymbol{i}_{abc}(x,t)/\partial x^2 = \boldsymbol{CL}\partial^2 \boldsymbol{i}_{abc}(x,t)/\partial t^2\end{cases} \tag{1}$$

where $\boldsymbol{u}_{abc}=[u_a \quad u_b \quad u_c]^T$ and $\boldsymbol{i}_{abc}=[i_a \quad i_b \quad i_c]^T$.

According to equation (1), the matrix CL or LC is not a diagonal matrix, and therefore the three phase voltages and currents are coupled. In order to simplify the solution procedure, transformation matrices $\boldsymbol{T}_u$ and $\boldsymbol{T}_i$ are usually adopted to transform phase components into mode components,

$$\boldsymbol{u}_{123}(x,t)=\boldsymbol{T}_u\cdot\boldsymbol{u}_{abc}(x,t),\ \boldsymbol{i}_{123}(x,t)=\boldsymbol{T}_i\cdot\boldsymbol{i}_{abc}(x,t) \tag{2}$$

Clarke transformation matrix is widely chosen to decouple three phase transmission lines [10-12]. The Clarke transformation matrix is defined as,

$$\boldsymbol{T}_u=\boldsymbol{T}_i=\boldsymbol{T}_{clarke}=\frac{1}{3}\begin{bmatrix}1 & 1 & 1\\ 2 & -1 & -1\\ 0 & \sqrt{3} & -\sqrt{3}\end{bmatrix} \tag{3}$$

where mode 1, 2 and 3 here are also known as zero mode, alpha mode and beta mode, respectively.

Under the assumption that the transmission lines are ideally transposed, the matrix $\boldsymbol{T}_{Clarke}\boldsymbol{CL}\boldsymbol{T}_{Clarke}^{-1}$ and $\boldsymbol{T}_{Clarke}\boldsymbol{LC}\boldsymbol{T}_{Clarke}^{-1}$ are diagonal matrices. In this case, the transmission line is completely decoupled. Therefore, the three phase transmission line can be treated as three single mode transmission lines.

B. Review for existing fault location algorithm

After decoupling the three phase transmission line into three independent single mode transmission lines, the existing natural frequency based fault location algorithm [10] selects a certain mode and calculates the fault location by,

$$d=(\theta_1+\pi)v/(4\pi f_d) \tag{4}$$

where f_d is the dominant frequency of the fault current signal of the certain mode, v is the wave speed of the traveling wave of the certain mode, and θ_1 is the angle of reflection coefficient of the certain mode at the line terminal.

The spectrum of the signal is extracted using the multiple signal classification [9]. There are frequency peaks in the spectrum, and the frequency corresponds to the first peak is selected to calculated the fault location, because it has the largest amplitude other than the fundamental frequency, and can be identified easily.

Note that the aforementioned calculations (including equation (4) itself) are all corresponding to a certain mode and are based on the assumption that the transmission line is fully decoupled. In the existing method, the three phase transmission line is decoupled using the standard Clarke transformation [5,9]. However, using the Clarke transformation matrix can just completely decouple the ideally transposed transmission lines, but probably not untransposed lines. In addition, the wave speed using the Clarke transformation may also be inaccurate. These factors may generate fault location errors in practice.

III. Proposed Method

In the proposed method, the three phase untransposed transmission lines will be fully decoupled. For general untransposed transmission line cases, the transmission line is asymmetrical. Therefore, applying the Clarke's matrix to decouple the transmission line may generate errors since the matrix $\boldsymbol{T}_{clarke}\boldsymbol{CL}\boldsymbol{T}_{clarke}^{-1}$ is not a diagonal matrix. To eliminate such errors, we need to find a new transformation matrix and then derive the connections of the corresponding mode networks during faults using the new transformation matrix.

A. Constructing the new transformation matrix

The eigenvalue decomposition for matrix $\boldsymbol{CL}$ and $\boldsymbol{LC}$ can be represented as,

$$\begin{cases}\boldsymbol{CL}=\boldsymbol{A}_i\boldsymbol{\lambda}\boldsymbol{A}_i^{-1}\\ \boldsymbol{LC}=\boldsymbol{A}_u\boldsymbol{\lambda}\boldsymbol{A}_u^{-1}\end{cases} \tag{5}$$

where $\boldsymbol{A}$ is the eigenvector matrix and λ is eigenvalue matrix. Let $T_i=A_i^{-1}$, $T_u=A_u^{-1}$, we can obtain,

$$\begin{cases}\boldsymbol{T}_i\boldsymbol{CL}\boldsymbol{T}_i^{-1}=\boldsymbol{T}_i\boldsymbol{A}_i\boldsymbol{\lambda}\boldsymbol{A}_i^{-1}\boldsymbol{T}_i^{-1}=diag([\lambda_1 \quad \lambda_2 \quad \lambda_3])\\ \boldsymbol{T}_u\boldsymbol{LC}\boldsymbol{T}_u^{-1}=\boldsymbol{T}_u\boldsymbol{A}_u\boldsymbol{\lambda}\boldsymbol{A}_u^{-1}\boldsymbol{T}_u^{-1}=diag([\lambda_1 \quad \lambda_2 \quad \lambda_3])\end{cases} \tag{6}$$

where $diag([\cdot])$ is a diagonal matrix with the diagonal $[\cdot]$.

Substitute equation (2) into equation (1),

$$\begin{cases}\partial^2 \boldsymbol{u}_{123}(x,t)/\partial x^2=\boldsymbol{T}_u\boldsymbol{LC}\boldsymbol{T}_u^{-1}\partial^2 \boldsymbol{u}_{123}(x,t)/\partial t^2\\ \partial^2 \boldsymbol{i}_{123}(x,t)/\partial x^2=\boldsymbol{T}_i\boldsymbol{CL}\boldsymbol{T}_i^{-1}\partial^2 \boldsymbol{i}_{123}(x,t)/\partial t^2\end{cases} \tag{7}$$

Or equivalently,

$$\begin{cases}\partial^2 i_j(x,t)/\partial x^2=\lambda_j\partial^2 i_j(x,t)/\partial t^2\\ \partial^2 u_j(x,t)/\partial x^2=\lambda_j\partial^2 u_j(x,t)/\partial t^2\end{cases} \tag{8}$$

where j = 1,2,3, and j represented the different transmission line modes.

The solution to equation (8) is,

$$u_j(x,t)=(f_j(t-x\sqrt{\lambda_j})+g_j(t+x\sqrt{\lambda_j})) \tag{9}$$

From equation (9), one can observe that the voltage $u_j(x,t)$

consists of two traveling waves that transmit to the opposite directions. The wave velocity is,

$$v_j = 1/\sqrt{\lambda_j} \tag{10}$$

where j =1,2,3.

B. Connections of mode networks during faults with the new transformation matrix

For different types of faults on the transmission line, it is necessary to choose appropriate modes to calculate the fault. The selection of a certain mode is according to the connection of mode networks during faults. Therefore, constructing the mode networks during faults with the new transformation matrix is essential to ensure applicability of (4) for fault location. To construct the mode networks during faults, an example test system is built in PSCAD/EMTDC. The example test system is a 500 kV system with a 200km untransposed transmission line. The tower is shown in Figure 2. The source parameters are shown in Table 1.

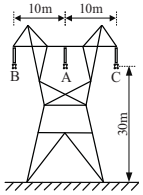

Figure 2. Tower structure of the transmission line

	Left source	Right source
Source impedance (per phase)	0.9+j0.377 (ohm)	0.5+j0.0628 (ohm)
Frequency	60 Hz	60 Hz
Phase angle	30°	0°

Table1. Sources parameters

For the transmission line, the new transform matrix can be calculated by (6) through eigenvalue decomposition,

$$\boldsymbol{T}_i = \begin{bmatrix} -0.5796 & -0.5772 & -0.5772 \\ 0.8434 & -0.3815 & -0.3815 \\ 0 & -0.7071 & 0.7071 \end{bmatrix}, \boldsymbol{T}_u = \begin{bmatrix} -0.5395 & -0.5964 & -0.5964 \\ 0.8163 & -0.4099 & -0.4099 \\ 0 & -0.7071 & 0.7071 \end{bmatrix}$$

One can actually observe that these two transformation matrices have very similar structures as the Clarke transformation matrix in (3): for the first row, the three elements are similar (corresponding to zero mode); for the second row, the last two elements are similar and the summation of all three elements is close to zero (corresponding to alpha mode); for the third row, the first element is zero and the summation of the next two elements are close to zero (corresponding to beta mode).

In the following part of this section, the new matrices will be used to obtain the connections of mode networks during different types of faults.

Define the three phase currents at fault location flowing into the fault as,

$$\boldsymbol{I}^f(t) = [I_a{}^f(t) \quad I_b{}^f(t) \quad I_c{}^f(t)]^T \tag{11}$$

The three phase voltages at fault location d is,

$$\boldsymbol{u}_d(t) = [u_a(d,t) \quad u_b(d,t) \quad u_c(d,t)]^T \tag{12}$$

Define the three mode currents at fault location flowing into the fault as,

$$\boldsymbol{I}_{123}{}^f(t) = [I_1{}^f(t) \quad I_2{}^f(t) \quad I_0{}^f(t)]^T \tag{13}$$

The three phase voltages at fault location d is,

$$\boldsymbol{u}_{d123}(t) = [u_1(d,t) \quad u_2(d,t) \quad u_3(d,t)]^T \tag{14}$$

1) Three phase fault

For a three phase fault, at the fault location, the relationship between the three phase currents and voltages is,

$$\boldsymbol{I}^f(t) = \boldsymbol{Y}_f \boldsymbol{u}_d(t) \tag{15}$$

where the fault admittance matrix is $\boldsymbol{Y}_f = diag([y_f \quad y_f \quad y_f])$, and y_f is the fault admittance per phase.

The fault admittance matrix in the mode network $\boldsymbol{Y}_{120}{}^f$ can be calculated as,

$$\boldsymbol{Y}_{120}{}^f = \boldsymbol{T}_i \boldsymbol{Y}_f \boldsymbol{T}_u^{-1} = \begin{bmatrix} 1.05y_f & 0.013y_f & 0.013y_f \\ 0.013y_f & 0.98y_f & -0.022y_f \\ 0.013y_f & -0.022y_f & 0.98y_f \end{bmatrix} \tag{16}$$

It can be observed that the off-diagonal components of the mode admittance matrix $\boldsymbol{Y}_{120}{}^f$ are small. Therefore, the off-diagonal elements are ignored, resulting in,

$$\boldsymbol{Y}_{120}{}^f = diag([1.05y_f \quad 0.98y_f \quad 0.98y_f]) \tag{17}$$

Hence, the distance can be calculated using all the three modes, and different modes will get the same fault location distance. In practice, since the source of the power system is typically close to symmetrical, the equivalent source inside mode 1 might be very small and therefore the current in mode 1 might also be small. Therefore, in general, mode 2 and mode 3 are better candidates compared to mode 1. The model network is shown in Figure 3.

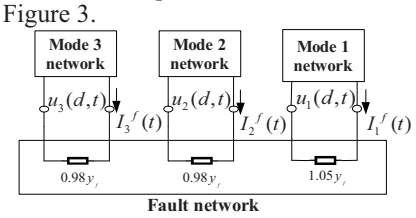

Figure 3. The model network for three phase fault

2) Phase to phase fault

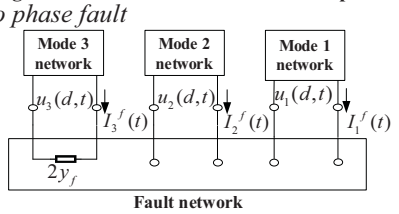

Figure 4. The fault network for phase to phase fault

Here we take phase B to phase C fault as an example. For phase B to phase C fault, at the fault location, the relationship between the three phase currents and voltages is,

$$\boldsymbol{I}^f(t) = \boldsymbol{Y}_f \boldsymbol{u}_d(t) = \begin{bmatrix} 0 & & \\ & y_f & -y_f \\ & -y_f & y_f \end{bmatrix} \boldsymbol{u}_d(t) \tag{18}$$

where y_f is the fault admittance between phase B and C.

Similarly, the fault admittance matrix in the mode network $\boldsymbol{Y}_{120}{}^f$ can be calculated as,

$$\boldsymbol{Y}_{120}{}^f = \boldsymbol{T}_i \boldsymbol{Y}_f \boldsymbol{T}_u^{-1} = \begin{bmatrix} -7.4\times10^{-32}y_f & -7.4\times10^{-32}y_f & -3.1\times10^{-16}y_f \\ 1.1\times10^{-29}y_f & 1.1\times10^{-29}y_f & 4.6\times10^{-14}y_f \\ 4.7\times10^{-16}y_f & 4.6\times10^{-16}y_f & 2y_f \end{bmatrix} \tag{19}$$

It can be observed that the matrix can be approximated as,

$$\boldsymbol{Y}_{120}{}^f = diag([0 \quad 0 \quad 2y_f]) \tag{20}$$

In this mode admittance matrix $\boldsymbol{Y}_{120}{}^f$, only the mode 3 diagonal component is non-zero. Hence, for phase B to phase C fault, the mode 3 is used to calculated the fault location and mode 1 and 2 are not with the information of fault location.

The model network is shown in Figure 4.

3) Double phase to ground fault

Here we take phase BC to ground fault as an example. For phase BC to ground fault, at the fault location, the relationship between the three phase currents and voltages is,

$$\boldsymbol{I}^f(t)=\boldsymbol{Y}_f\boldsymbol{u}_d(t)=diag([0 \quad y_f \quad y_f])\boldsymbol{u}_d(t) \tag{21}$$

where y_f is the fault admittance of phase B and C.

Similarly, the fault admittance matrix in the mode network $\boldsymbol{Y}_{120}{}^f$ can be calculated as,

$$\boldsymbol{Y}_{120}{}^f=\boldsymbol{T}_i\boldsymbol{Y}_f\boldsymbol{T}_u^{-1}=\begin{bmatrix} 0.67y_f & 0.44y_f & 2.9\times10^{-16}y_f \\ 0.44y_f & 0.23y_f & 2.35\times10^{-14}y_f \\ 1.2\times10^{-16}y_f & 1.3\times10^{-16}y_f & y_f \end{bmatrix} \tag{22}$$

It can be observed that the matrix can be approximated as,

$$\boldsymbol{Y}_{120}{}^f=\begin{bmatrix} 0.67y_f & 0.44y_f & 0 \\ 0.44y_f & 0.23y_f & 0 \\ 0 & 0 & y_f \end{bmatrix} \tag{23}$$

The model network is shown in Figure 5.

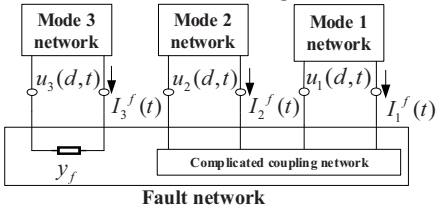

Figure 5. The fault network for double phase to ground fault

The mode admittance matrix $\boldsymbol{Y}_{120}{}^f$ of phase BC to ground fault is more complicated than that of the phase B to phase C. Similar as the phase B to phase C fault, the mode 3 can also be selected to calculate the fault location. However, mode 1 and 2 are coupled and the connection of the mode network can be very complicated. For these two modes each mode current is related to the other mode voltage, which is the phenomenon of model mixing [10]. Therefore, mode 1 and 2 are not selected to calculate the fault location.

4) Single phase to ground fault

Here we take phase A to ground fault as an example. For phase A to ground fault, at the fault location, the relationship between the three phase currents and voltages is,

$$\boldsymbol{I}^f(t)=\boldsymbol{Y}_f\boldsymbol{u}_d(t)=diag([y_f \quad 0 \quad 0])\boldsymbol{u}_d(t) \tag{24}$$

where y_f is the fault admittance of phase A.

Similarly, the fault admittance matrix in the mode network $\boldsymbol{Y}_{120}{}^f$ can be calculated as,

$$\boldsymbol{Y}_{120}{}^f=\boldsymbol{T}_i\boldsymbol{Y}_f\boldsymbol{T}_u^{-1}=\begin{bmatrix} 0.34y_f & -0.49y_f & -5.2\times10^{-16}y_f \\ -0.49y_f & 0.71y_f & 7.5\times10^{-16}y_f \\ -8.7\times10^{-18}y_f & 1.3\times10^{-17}y_f & 1.4\times10^{-32}y_f \end{bmatrix} \tag{25}$$

It can be observed that the matrix can be approximated as,

$$\boldsymbol{Y}_{120}{}^f=\begin{bmatrix} 0.34y_f & -0.49y_f & 0 \\ -0.49y_f & 0.71y_f & 0 \\ 0 & 0 & 0 \end{bmatrix} \tag{26}$$

The model network is shown in Figure 6.

For the single phase to ground fault, similar as the double phase to ground fault, the mode 1 and 2 have mode mixing phenomena . For these two modes each mode current is related to the other mode voltage and the connection between them is complicated. On the other hand, mode 3 is an open circuit and therefore it does not contain any fault component. In fact, the existing method also has the similar mode mixing issue. Present solution is to use the average wave speed of alpha mode and zero mode as the approximate wave speed and approximate the fault location [10,13], but the method may still encounter errors during extreme scenarios. As this is a common issue in present natural frequency based fault location approaches, in this paper, we will not discuss the fault location results for single line to ground faults.

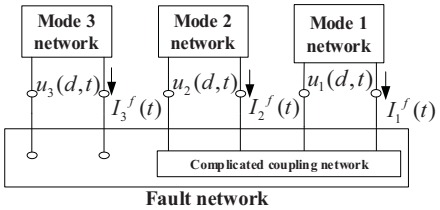

Figure 6. The fault network for single phase to ground fault

IV. Numerical Experiments

To verify this proposed method, an example test system is built in PSCAD/EMTDC. The transmission line is a 500 kV, 200km untransposed transmission line with tower structures shown in Figure 2. The fault location is calculated using three phase current signals at one terminal. The sampling rate is 100 kilo-samples per second.

As mentioned in section III.B, new transformation matrix has similar structure as the Clarke transformation matrix: mode 1, 2 and 3 using the new transformation matrix correspond to mode zero, alpha and beta using the Clarke transformation matrix. From equation (10), the alpha mode wave speed and beta mode wave speed are $2.9325\times10^8\,m/s$ and $2.9377\times10^8\,m/s$, respectively; the mode 2 wave speed and mode 3 wave speed are $2.9401\times10^8\,m/s$ and $2.9300\times10^8\,m/s$, respectively. The error between the proposed method wave speed and existing method wave speed is about 0.26%.

From the new transformation matrix, it is obvious to find that mode 3 is exactly the same as the Clarke's transformation beta mode, so the dominant frequency extracted by the two modes are exact the same. Here, we verify the dominant frequency difference between the mode 2 and alpha mode through three phase ABC faults at different locations with different fault impedances. The absolute differences of the dominant frequencies are depicted in Figure 7. The maximum absolute difference is around 0.4Hz. This frequency difference contributes to the fault location error of the existing approach.

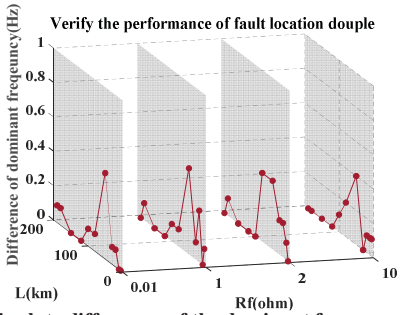

Figure 7. Absolute differences of the dominant frequency between the proposed method and the existing method

Next, the performance of the proposed method is compared to the existing dominant frequency fault location method using the Clarke transformation. Here, we will show the performance during three phase faults, BC faults and BCG faults to verify the effectiveness of the proposed method. Different fault distance L from 5km to 190km and fault impedance R_f from 0.01 to 10 ohm are considered. For each case, the fault location distance error of the proposed method (red lines in the Figure), and the existing method error (blue lines in the Figure) are provided.

A. Test case 1: three phase fault

This test case studies a group of low impedance three phase

faults with different fault location distance L (from 5km to 190km) and different fault impedances R_f (0.01ohm, 1ohm, 2ohm, 10ohm). The fault location errors of the proposed method and the existing method are shown in Figure 8. It can be observed that the proposed method presents higher accuracy than the existing method. According to Figure 8, the maximum error of proposed method is lower than that of the existing method (about 0.20%).

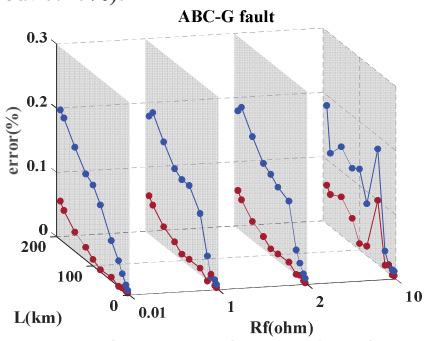

Figure 8. Results of three phase faults, variable fault location

B. Test case 2: phase B to phase C fault

This test case studies a group of low impedance phase B to phase C faults with different fault location distance L (from 5km to 190km) and different fault impedances R_f (0.01ohm, 1ohm, 2ohm, 10ohm). The fault location errors of the proposed method and the existing method are shown in Figure 9. It can be observed that the proposed method presents higher accuracy than the existing method. According to Figure 9, the maximum error of proposed method is lower than that of the existing method (about 0.25%).

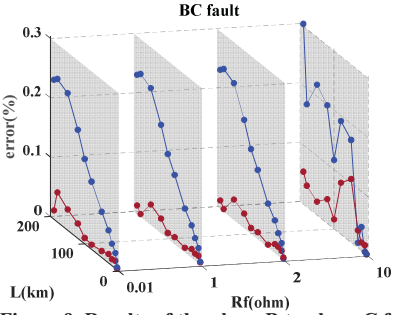

Figure 9. Results of the phase B to phase C fault

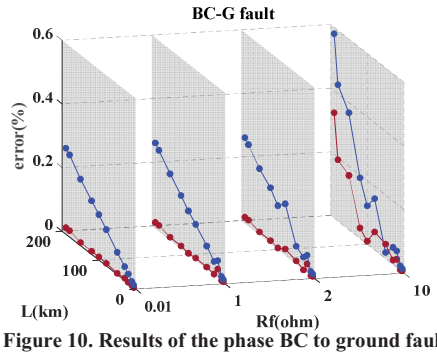

Figure 10. Results of the phase BC to ground fault

C. Test case 3: phase BC to ground fault

This test case studies a group of low impedance phase BC to ground faults with different fault location distance L (from 5km to 190km) and different fault impedances R_f (0.01ohm, 1ohm, 2ohm, 10ohm). The fault location errors of the proposed method and the existing method are shown in Figure 10. It can be observed that the proposed method presents higher accuracy than the existing method. According to Figure 10, the maximum error of proposed method is lower than that of the existing method (about 0.25%).

D. Discussions

In the numerical experiments, the proposed method focuses on the phase faults occurring on the transmission line, and it has more accurate fault location results than the existing method. The improvement of the fault location accuracy could be valuable especially when applied to long transmission lines with severe scenarios of line asymmetry (the improvement could be in the order of several kilometers with long transmission lines).

On the other hand, because of the mode mixing phenomenon for the single line ground fault discussed in section III, there are still challenges to obtain very accurate fault location results (like the results in Figure 8-10). More accurate fault location method will be discussed in future publications.

V. Conclusion

This paper proposes a natural frequency based fault location method on untransposed transmission lines. Unlike the existing natural frequency based fault location method, the proposed method does not require the geometrically symmetrical assumption of transmission lines. A new phase to model transformation matrix is constructed and the connections of mode networks during fault with the new transformation matrix are derived. Numerical experiments prove that the proposed method has higher accuracy compared to the existing method during phase faults with different fault types, locations and impedances. The way to systematically solve the mode mixing phenomenon during single phase to ground faults will be studied in future publications.

References

[1] "IEEE Guide for Determining Fault Location on AC Transmission and Distribution Lines", *IEEE Std C37. 114-2014.*

[2] Y. Liu, B. Wang, X. Zheng, D. Lu, M. Fu and N. Tai, "Fault Location Algorithm for Non-Homogeneous Transmission Lines Considering Line Asymmetry", *IEEE Trans. Power Del.*, 2020, early access.

[3] Y. Liu, A. P. Meliopoulos, Z. Tan, L. Sun and R. Fan, "Dynamic State Estimation-Based Fault Locating on Transmission Lines", *IET Gener. Transm. Distrib.*, Vol. 11, No. 17, pp. 4184-4192, Nov. 2017.

[4] D. Lu, Y. Liu, Q. Liao, et al, "Time-domain Transmission Line Fault Location Method with Full Consideration of Distributed Parameters and Line Asymmetry", *IEEE Trans. Power Del.*, early access.

[5] S. M. Brahma and A. A. Girgis, "Fault Location on a Transmission Line Using Synchronized Voltage Measurements," *IEEE Trans. Power Del.,* Vol. 19, No. 4, pp. 1619-1622, Oct. 2004.

[6] C. Zhang, G. Song, T. Wang and L. Yang, "Single-Ended Traveling Wave Fault Location Method in DC Transmission Line Based on Wave Front Information," *IEEE Trans. Power Del.,* Vol. 34, No. 5, pp. 2028-2038, Oct. 2019.

[7] Azizi, S., Sanaye-Pasand, M., Abedini, M., et al.: 'A Traveling Wave-Based Methodology for Wide-Area Fault Location in Multiterminal DC Systems,' *IEEE Trans. Power Deliv.,* Vol 29, No. 6, pp. 2552–2560, Aug. 2014.

[8] Y. Liu, S. Meliopoulos, N. Tai, L. Sun and B. Xie, "Protection and Fault Locating Method of Series Compensated Lines by Wavelet Based Energy Traveling Wave", in *IEEE PES General Meeting (PESGM)*, 2017.

[9] Z. He, K. Liao, X. Li, et al., "Natural Frequency-Based Line Fault Location in HVDC Lines", *IEEE Trans. Power Del.,* Vol. 29, No. 2, pp. 851-859, Jul. 2014.

[10] L.Y. Wu, Z. He, Qian Q. "A New Single Ended Fault Location Technique Using Traveling Wave Natural Frequencies", *IEEE PES Asia Pacific Power Energy Engineering Conf., APPEEC09, Wuhan, China, 2009.*

[11] S. Lin, Z. He, X. Li, Q. Qian, "Traveling Wave Time-Frequency Characteristic-Based Fault Location Method for Transmission Lines", *IET Gener. Transm. Distrib.,* Vol. 6, No. 8, pp. 764-772, Aug 2012.

[12] Z. He, X. Li and S. Chen, "A Traveling Wave Natural Frequency-Based Single-Ended Fault Location Method with Unknown Equivalent System Impedance", *Int. Trans. Electr. Energ. Syst.,* Vol.26, No.3, pp.509-524, Mar. 2015.

[13] G. Song, X. Chu, et al., "A Fault-Location Method for VSC-HVDC Transmission Lines Based on Natural Frequency of Current", *Elect. Power Energy Syst* ,Vol.63, pp. 347-352 , Dec. 2014.